Journal of
Nanoscience and Nanotechnology
Vol. 11, 1–5, 2011

Effect of Annealing Temperature on the Structural and Magnetic Properties of Co-Doped TiO_2 Nanoparticles via Complex-Polymer Sol–Gel Method

Masoud Karimipour[1, 2, 3, *], J. Magnus Wikberg[4], Nasser Shahtahmasebi[1, 2], Mahmood Rezaee Rokn Abad[1, 2], M. M. Bagheri-Mohagheghi[5], and Peter Svedlindh[4]

[1] *Department of Material physics, Uppsala University, Box 516, SE-75120, Uppsala, Sweden*
[2] *Department of Physics, Faculty of Basic Science, Ferdowsi University, Mashhad, Iran*
[3] *Nanotechnology Lab, Nano Research Center, Ferdowsi University, Mashhad, Iran*
[4] *Department of Engineering Sciences, Uppsala University, Box 534, SE-75121, Uppsala, Sweden*
[5] *School of Physics, Damghan University, Damghan, Iran*

Co-doped TiO_2 nanoparticles were synthesized via non hydrous complex-polymer sol–gel method. A series of Co_x:$Ti_{1-x}O_2$ samples with $x = 0.01$, 0.03, 0.05, 0.08 and 0.10, were prepared and subsequently annealed at 400°, 600° and 800 °C. Structural and magnetic properties of Co_x:$Ti_{1-x}O_2$ have been studied by means of X-ray diffraction and DC magnetometry. All samples annealed at 400 °C show a paramagnetic behavior with an average grain size of 11 nm. With increasing annealing temperatures a complete crystallization is seen with growth of the cluster size up to 31 nm with clear evidence of a presence of $CoTiO_3$. For all concentrations and annealing conditions no sign of a metallic phase, even at $x = 0.10$, is seen.

Keywords: Diluted Magnetic Semiconductors, Sol–Gel Process, X-ray Diffraction, DC Magnetometry, Ferromagnetism in Semiconductor.

RESEARCH ARTICLE

1. INTRODUCTION

Diluted magnetic semiconductors (DMS) are essential materials for the development of spintronic devices, which simultaneously utilize the charge and spin of the carriers. By Doping with transition metal (TM) ions into cation sites in the host semiconductor lattice, Ferromagnetic properties are introduced into nonmagnetic semiconductors.[1] Since, Titanium oxide is one of the most important candidate for multifunctional applications in electronic, optic, photo catalytic treatments and hydrogen storage,[2] TM doped TiO_2 in the nano scale has been investigated by many groups.[3–8] But the understanding of the connection between the structural and magnetic properties of TiO_2 doped with TM-ions is still under debate.[9] This applies especially to the case of Co-doped TiO_2 which has been reported to have a strong ferromagnetic moment at room temperature.[10–11] Many techniques such as pulsed laser deposition (PLD),[12–15] molecular beam epitaxy (MBE),[16, 17] reactive co-sputtering,[18–21] spin coating and dip-coating[22] have been employed for making Co-doped TiO_2 thin films and nano structures. The chemical nature of the ferromagnetic phase is a subject of discussion. Since most of the above film synthesis methods are performed under vacuum or low oxygen pressure conditions, the formation of metallic cobalt clusters, giving rise to ferromagnetism, must be considered. Particularly, when chemical synthesis methods are used, the synthesis parameters need to be controlled to prohibit the metallic phase formation in the TiO_2 network. The solubility of Co in TiO_2 depends on the method of preparation can be different signifcantly.[23] Recently, a polymerizing-complexing (PC) combustion method, which is a modified Pechini process,[24–26] without any precipitation, has been used for preparation of semiconductor nano-particles such as SnO_2. This method consists of using a variety of Organic fuels such as citric acid (CiAc), urea, hydrazine, EDTA, acetyl acetone (AcAc) and ethylene glycol as complexing or polymerization agents.[27, 28] Indeed, the PC method results in a more homogeneous fine powder than any other technique with immobilization of metal-chelate complex. In this work, Co-doped TiO_2 nanoparticles have been synthesized using a metal-organic precursor and non hydrous solvent. The main goal of the present study is to

*Author to whom correspondence should be addressed.

produce nanoparticles of controllable size without a metallic phase formation, for high and low values of Co-doping concentration.

2. EXPERIMENTAL DETAILS

The preparation of the $(Co_xTi_{1-x})O_2$ nano powders by the PC sol–gel method is summarized in a flowchart shown in Figure 1. The initial sol was prepared by a precursor solution, titanium (IV) isopropoxide ($Ti(OCH(CH_3)_2)_4$: Sigma-Aldrich), diluted in absolute ethanol (99.99%, Sigma-Aldrich) in volumetric ratio of 1:3. Afterwards, the dopant solution which contained the $CoCl_2$:$6H_2O$ was dissolved in 10 cc of absolute ethanol. Then the dopant solution was added to the precursor solution and after a few seconds citric acid (Ci Ac) and AcAc were added to the initial solution. The resulting transparent mixture was stirred and dissolved at room temperature. From experimental point of view, the most important part was forming a transparent sol containing titanium iso-propoxide and hydrous mineral material. Worth noticing is that titanium iso-propoxide reacts intensively with water and precipitates. The obtained solution was refluxed at 120 °C for 6 h in an oil bath and was let to cool down to get a transparent sol. In order to have a uniform gel with a polymerized network and to evaporate the solvent, the sol was kept at 80 °C for 18 h in an oil bath. In the last step of the sol–gel process, the wet gel was fully dried by direct heating at 200 °C for 1 h. The resulting powders had a black color. A number of solutions with different Co doping concentrations were prepared. The final powders contain 1, 3, 5, 8 and 10% atom of Co. As a final step the powders where annealed for 1 h at 400°, 600° or 800 °C. X-ray diffraction (XRD) was used for investigating of the phase formation and size distribution of particles. The measurements were performed at room temperature using a Bruker D8 diffractometer with Cu Kα ($\lambda = 1.54056$ Å) radiation. Bragg diffraction position (θ), Full Width at Half Maximum (FWHM), crystal structure and crystallographic growth planes were extracted from the data. The average size of the nanoparticles was determined through the Scherrer formula.[29] DC magnetization measurements were performed in a Quantum Design MPMS-XL system. Zero field cooled (ZFC) and field cooled (FC) magnetization were measured under an applied field of 500 Oe between 10–400 K. Magnetization (M) versus field (H) measurements were performed at 10 K between ±30 kOe.

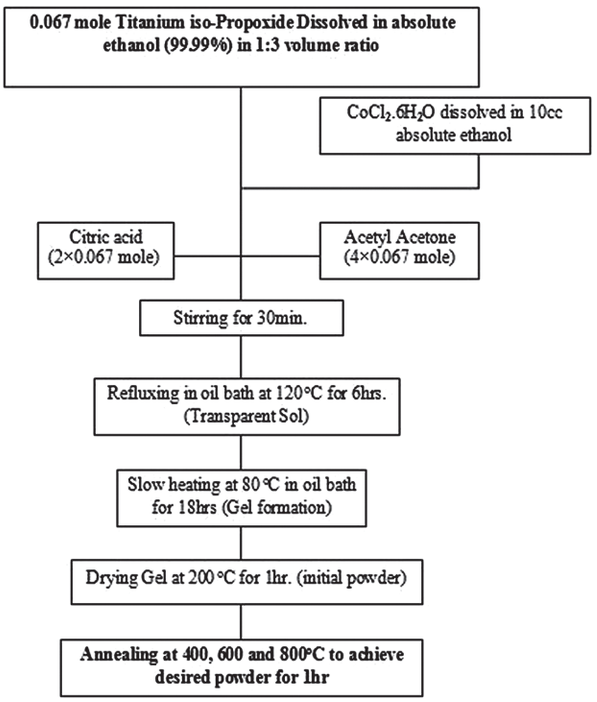

Fig. 1. Flowchart of the sol–gel process.

3. RESULTS AND DISCUSSION

3.1. Structural Characterization

TiO_2 has three main crystalline structures, namely, Rutile ($a = b = 4.584$ Å; $c = 2.953$ Å), Anatase ($a = b = 3.782$ Å; $c = 9.502$ Å) and Brookite ($a = 5.436$ Å; $b = 9.166$ Å; $c = 5.135$ Å), among which Rutile is the most stable one. Structures of both Rutile and Anatase phases are tetragonal and can be regarded as a network of coordinated TiO_6 octahedral. Depending on the method of preparation and the materials used,[30–32] Anatase forms at 200–450 °C and has a phase transition to Rutile around 550–700 °C. Therefore, the temperatures 400 °, 600° and 800°C were chosen for annealing the powders. The grained powders were annealed for 1 h in glassy boats in an electric cubic furnace. After annealing, the color of the powders varied from yellow for the 1% Co-doped powder to dark green for the 10% Co-doped powder. The average weight reduction due to annealing was $55 \pm 1\%$ for 400 °C, $80 \pm 0.1\%$ for 600 °C and $80.3 \pm 0.1\%$ for the 800 °C powder sample.

The XRD results for powders annealed at 400 °C are shown in Figure 2(a).

For $x = 0.05$, The Anatase and Rutile phases co-exist with a significant peak broadening due to non-Uniform strain. This points to the fact that the structure of the nanoparticles has an Amorphous background, which can be due to the presence of H_2O and carbon compounds. The (101)-plane for Anatase and (110)-plane for Rutile are the main diffraction planes seen in the figure. There is no diffraction peak that can be attributed to metallic Co. However, the Co atoms affect the structure because they contribute to strain in the in the TiO_2 lattice, making the intensity of the Rutile (110) diffraction peak to vanish and instead paving the way for formation of Brookite phase for $x > 5$%-at. The XRD results for (101) diffraction peak of

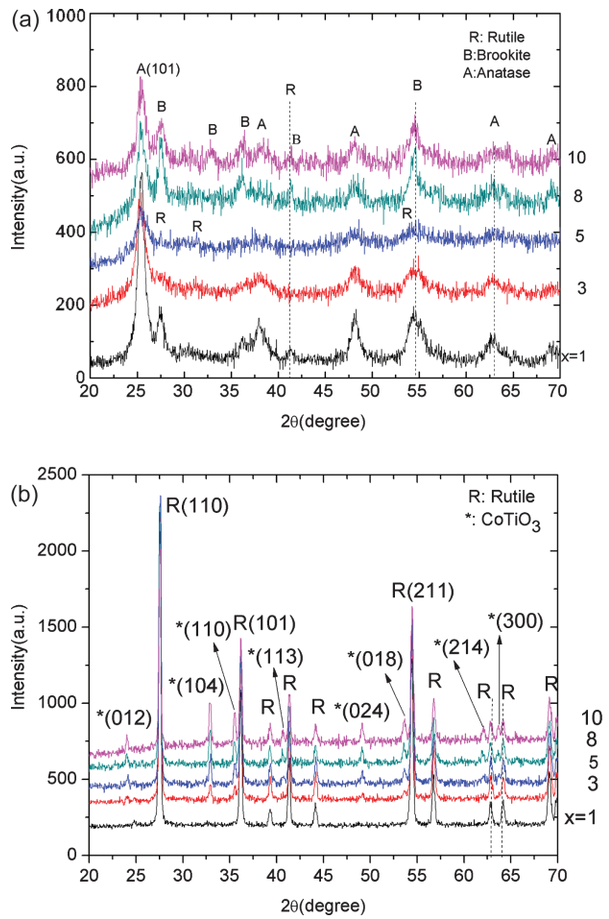

Fig. 2. (a) XRD data at room temperature for samples, $x = 0.01$, 0.03, 0.05, 0.08 and 0.10, annealed at 400° and (b) XRD data at room temperature for samples, $x = 0.01$, 0.03, 0.05, 0.08 and 0.10, annealed at 800 °C.

the Anatase phase after annealing at 400 °C are summed up in Table I. The peak intensity decreases with increasing Co-concentration up to $x = 0.05$ but with further increasing concentration the peak intensity increases due to formation of the Brookite phase. Also, a shift in peak position is observed due to uniform strain in the structure. Structural defects and insertion of Co in the TiO_2 structure are the origin of the strain. The mean size of the nanoparticles for the Anatase phase is given in Table I, indicating an expansion of the lattice with increasing Co concentration. In Figure 3 the Anatase to Rutile phase transition when increasing the annealing temperature from 400° to 800 °C for $x = 0.10$ is seen. By increasing the annealing temperature from 400° to 800 °C, a rapid mass loss of the powder occurs due to evaporation and removing of organic additives such as citric acid and Acetyl Acetone. It is also evident that the lattice structures at 800° and 600 °C are the same and by increasing the annealing temperature from 600° to 800 °C Rutile and $CoTiO_3$ crystallization are favored. It is worth noticing that with increasing the

Table I. XRD results with the 2 values for the (101) diffraction peak and tetragonal crystal structure. (2 θ: Bragg diffraction angle; FWHM: Full Width at Half Maximum and d: atomic plane distance).

x	2 θ (deg)	D (Å)	FWHM (deg)	Mean grain size (nm)	Crystal structure
1	25.42	3.50	0.759	11.2	tetragonal
3	25.40	3.50	0.947	9	tetragonal
5	25.28	3.52	0.75	11.3	tetragonal
8	25.29	3.52	0.709	12	tetragonal
10	25.36	3.51	0.67	12	tetragonal

annealing temperature the intensity increase for the (211)-plane is much higher than for the (110)-plane in Rutile. As seen in Figure 2(b), when annealing the powders at 800 °C, the Anatase phase completely disappears and the powder exhibits a polycrystalline structure with the Rutile and $CoTiO_3$ phases.

The main planes for crystalline growth of the Rutile phase are the (110), (101) and (211) planes. With increasing Co concentration hexagonal $CoTiO_3$ is formed as evidenced by the appearance of the (104),(110) and (012) diffraction peaks. It is worth noticing that both the Rutile and $CoTiO_3$ phases have grown mostly in the (110) plane. It shows that the polymer agent (AcAc) has connected the chemical bonds of free complexes in this plane which can be modified by changing the concentration of the polymer and complex agents. Table II shows the XRD parameters for $Cox:Ti_{1-x}O_2$ with $x = 0.01$, 0.03, 0.05, 0.08 and 0.10. Due to lattice parameter mismatch between the Rutile and $CoTiO_3$ phases, there are uniform and non-uniform strains which cause both a change in lattice parameters and in Bragg peak positions. Also, with increasing Co concentration, the intensity of the (110) peak decrease while the (101) and (211) peaks show increase in intensity. The full width at half maximum (FWHM) values decrease for all three diffraction peaks with increasing x. This indicates

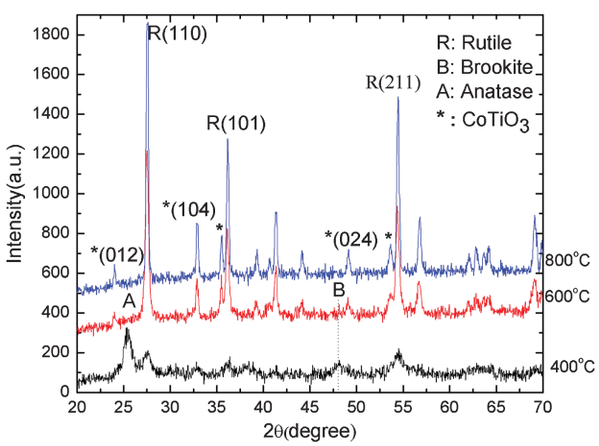

Fig. 3. XRD data at room temperature for $x = 10$, annealed at 400° (black), 600° (red) and 800 °C (blue). Indications for the 2 θ positions for Rutile (R), Brookite (B), Anatase (A) and $CoTiO_3$ (*).

RESEARCH ARTICLE

Table II. XRD results with parameters for powders annealed at 800 °C.

x	hkl	2 θ (deg)	D (Å)	FWHM (deg)	Mean grain size (nm)	Crystal structure
1	110	27.52	3.24	0.281	30	tetragonal
	101	36.15	2.48	0.276	31	tetragonal
	211	54.42	1.68	0.316	30	tetragonal
3	110	27.55	3.23	0.283	30	tetragonal
	101	36.19	2.48	0.287	30	tetragonal
	211	54.44	1.68	0.318	29	tetragonal
5	110	27.56	3.23	0.278	31	tetragonal
	101	36.20	2.48	0.288	30	tetragonal
	211	54.47	1.68	0.308	30	tetragonal
	104	32.94	2.71	0.237	37	Hexagonal
8	110	27.52	3.24	0.275	31	tetragonal
	101	36.16	2.48	0.273	32	tetragonal
	211	54.43	1.68	0.305	31	tetragonal
	104	32.91	2.72	0.253	34	Hexagonal
10	110	27.54	3.24	0.279	31	tetragonal
	101	36.17	2.48	0.288	32	tetragonal
	211	54.44	1.68	0.296	31	tetragonal
	104	32.90	2.72	0.253	34	Hexagonal

a growth of crystalline Rutile which is accompanied by an improved crystalline orientation. Figure 4 shows these results for changing the mean size of nanoparticles as a result of rotation of preferred growing plane of Rutile structure (left axis) and change in a-axis of $CoTiO_3$ unit cell (right axis). For $x = 0.10$, a significant increase in the average size of particle for (211) plane besides a decrease in average size for (101) and (110) planes-caused by increasing in lattice parameter of $CoTiO_3$ shows a clear rotation of crystalline growth plane of Rutile.

3.2. Magnetic Properties

As seen in Figure 5, all samples annealed at 400 °C exhibit a paramagnetic (PM) behavior. Whereas the 800 °C

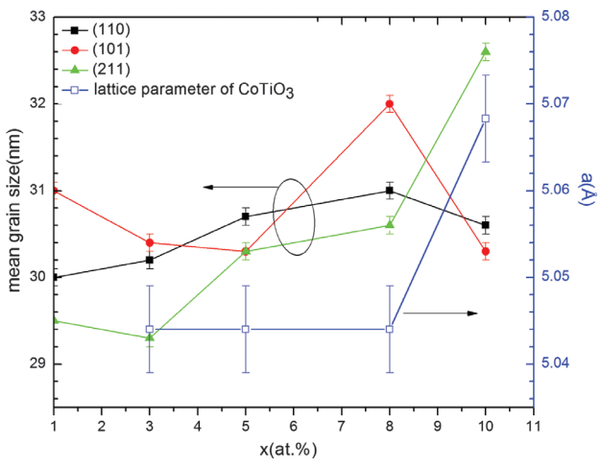

Fig. 4. Mean size of nanoparticles (left) and a-lattice parameter of $CoTiO_3$ phase (right) versus Co concentration annealed at 800 °C calculated for three planes of Rutile phase.

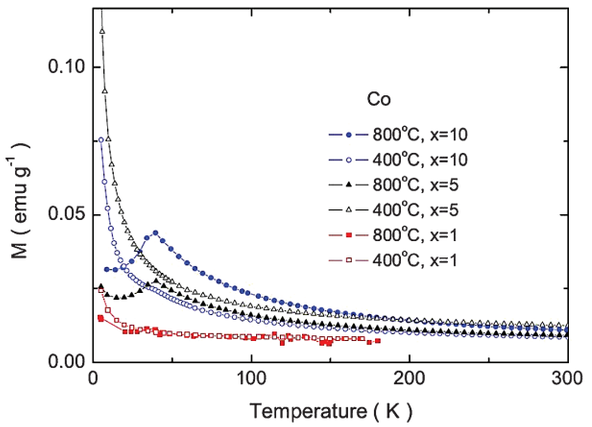

Fig. 5. Field Cooled (FC) magnetization under an applied field of 500 Oe, for Co_xTiO_2 with $x = 1$, 5 and 10 annealed either at 400° or 800 °C.

samples all show, along with a PM tale at low temperatures, features related to an antiferromagnetic (AFM) phase transition at a Néel temperature (T_N) of 40 K. It should be noted that even for $x = 0.01$ a kink in the FC magnetization is observed at 40 K. No difference could be detected between the FC and ZFC (not shown) curves for all concentrations and annealing temperatures. In the magnetization (M) versus field (H) measurements shown in Figure 6(a) linear field dependence is observed except for $x > 5$ annealed at 800 °C which display an increased slope at the highest fields. The AFM behavior in FC observed Figure 5 is attributed to the formation of $CoTiO_3$, also seen in the XRD measurements, which has a $T_N = 38$ K.[33] The formation of this phase could possibly also explain the deviation from a linear field dependence in the magnetization versus field curves (cf. Fig. 6) for powders annealed at 800 °C with $x = 0.05$.

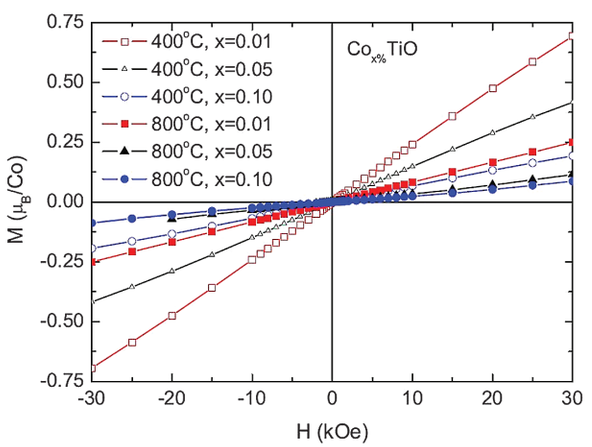

Fig. 6. Magnetization (M) versus field (H) at 10 K for $x = 1$, 5 and 10 annealed at 400° and 800 °C.

RESEARCH ARTICLE

4. CONCLUSION

Co-doped TiO_2 nanoparticles were synthesized successfully via the PC sol–gel method. Without formation of metallic clusters. Titanium isopropoxide was used as precursor, while CiAc and AcAc were used as complex agent and polymer agent, respectively. AcAc = Ti:CiAc = Ti:4:2 mole ratios were chosen to prohibit agglomeration of nanoparticles. A phase coexistence of Rutile and Anatase phase is seen in XRD for the low annealing temperatures (400 °C and 600 °C) and there was no detected phase for Cobalt. Through variation of the mole ratios of AcAc and CiAc it may be possible to consider different crystalline structures and higher crystallization which is deferred for future works. At 800 °C annealing temperature the Rutile phase with a preferential (110) plane is a single phase for TiO_2. No metallic phase of Co was detected for any concentration or annealing temperatures. For all concentrations, the 400 °C samples display smallest particle sizes, all exhibiting a paramagnetic behavior. The nanoparticles grow in size with increasing annealing temperatures to 31 nm for the highest annealing temperature, forming AFM $CoTiO_3$ clusters visible both in XRD and magnetometry.

Acknowledgments: Masoud Karimipour would like to thank Professor Bjorgvin Hjorvarsson and Dr. vassilios kapaklis in department of Material physics, Uppsala University, Sweden- for fruitful discussions. J. Magnus Wikberg and Peter Svedlindh would like to thank the Swedish Research Council (VR) and the Knut and Alice Wallenberg Foundation (KAW) for financial support.

References and Notes

1. J.-P. Xu, L. Li, L.-Y. Lv, X.-S. Zhang, X.-M. Chen, J.-F. Wang, F.-M. Zhang, W. Zhong, and Y.-W. Du, *J. Chin. Phys. Lett.* 26, 097502 (**2009**).
2. I. P. Suzdaleva, V. E. Prusakova, Y. V. Maksimova, V. K. Imshennika, S. V. Novochikhina, E. A. Gudilinb, A. V. Grigorevab, K. L. Dubovab, S. S. Abramchukb, Yu. D. Tretyakovb, I. S. Lyubutinc, and K. D. Frolo, *J. Nanotechnologys In Russia* 5, 3 (**2010**).
3. G. U. von Oertzena and A. R. Gerson, *J. Physics and Chemistry of Solids* 68, 324 (**2007**).
4. Y. Matsumoto, R. Takahashi, M. Murakami, T. Koida, X. J. Fan, T. Hasegawa, T. Fukumura, M. Kawasaki, S.Y. Koshihara, and H. Koinuma, *Jpn. J. Appl. Phys.* 40, L1204 (**2001**).
5. L. A. Balagurov, S. O. Klimonsky, S. P. Kobeleva1, A. S. Konstantinova, A. Forlov, N. S. Perov, A. Sapelkin, and D. G. Yarkin, *J. Phy.: Condens. Matter* 18, 10999 (**2006**).
6. N. H. Hong, J. Sakai, and W. Prellier, *Phys. Rev. B* 70, 195204 (**2004**).
7. R. Alexandrescu, I. Morjan, M. Scarisoreanu, R. Birjega, E. Popovici, I. Soare, L. Gavrila-Florescu, I. Voicu, I. Sandu, F. Dumitrache, G. Prodan, E. Vasile, and E. Figgemeier, *Thin Solid Films* 515, 8438 (**2007**).
8. P. Lianos, *Adv. Sci. Lett.* 1, 128 (**2008**).
9. V. Bilovol, A. M. M. Navarro, W. T. Herrera, D. R. Sanchez, E. M. Baggio-Saitovich, C. E. R. Torres, F. H. Sanchez, and A. F. Cabrera, *Hyper_ne Interact* 195, 155 (**2010**).
10. N. Akdogan, A. Nefedov, H. Zabel, K. Westerholt, H. W. Becker, C. Somsen, S. Gok, A. Bashir, R. Khaibullin, and L. Tagirov, arxiv. 9, 0807.1555 (**2008**).
11. J. D. Bryan, S. M. Heald, S. A. Chambers, and D. R. Gamelin, *J. Am. Chem.* 126, 11640 (**2004**).
12. Y. Matsumoto, *Science* 294, 1003 (**2001**).
13. D. H. Kim, J. S. Yang, K. W. Lee, S. D. Bu, T. W. Noh, S. J. Oh, Y. W. Kim, J. S. Chung, H. Tanaka, H. Y. Lee, and T. Kawai, *Appl. Phys. Lett.* 81, 2421 (**2002**).
14. Y. Yamada, H. Toyosaki, A. Tsukazaki, T. Fukumura, K. Tamura, Y. Segawa, K. Nakajima, T. Aoyama, T. Chikyow, T. Hasegawa, H. Koinuma, and M. Kawasaki, *J. Appl. Phys.* 96, 5097 (**2004**).
15. J. Li, O. H. Sow, S. X. Rao, C. K. Ong, and D. N. Zheng, *Eur. Phys. J. B* 32, 471 (**2003**).
16. S. A. Chambers, S. Thevuthasan, R. F. C. Farrow, R. F. Marks, J. U. Thiele, L. Folks, M. G. Samant, A. J. Kellock, N. Ruzycki, D. L. Ederer, and U. Diebold, *Appl. Phys. Lett.* 79, 3467 (**2001**).
17. T. C. Kaspar, T. Droubay, C. M. Wang, S. M. Heald, A. S. Lea, and S. A. Chambers, *J. Appl. Phys.* 97, 073511 (**2005**).
18. W. K. Park, R. J. Ortega-Hertogs, J. S. Moodera, A. Punnoose, and M. S. Seehra, *J. Appl. Phys.* 91, 8093 (**2002**).
19. A. Punnoose, M. S. Seehra, W. K. Park, and J. S. Moodera, *J. Appl. Phys.* 93, 7867 (**2003**).
20. D. H. Kim, J. S. Yang, K. W. Lee, S. D. Bu, D. W. Kim, T. W. Noh, S. J. Oh, Y. W. Kim, J. S. Chung, H. Tanaka, H. Y. Lee, T. Kawai, J. Y. Won, S. H. Park, and J. C. Lee, *J. Appl. Phys.* 93, 6125 (**2003**).
21. M. Murakami, Y. Matsumoto, T. Hasegawa, P. Ahmet, K. Nakajima, T. Chikyow, H. Ofuchi, I. Nakai, and H. Koinuma, *J. Appl. Phys.* 95, 5330 (**2004**).
22. M. Subramanian, S. Vijayalakshmi, S. Venkataraj, and R. Jayavel, *Thin Solid Films* 516, 3776 (**2008**).
23. M. Fleischhammer, M. Panthofer, and W. Tremel, *J. Solid State Chemistry* 182, 942 (**2009**).
24. M. M. Bagheri-Mohagheghi, N. Shahtahmasebi, M. R. Alinejada, A. Yousse, and M. Shokooh-Saremi, *Physica B* 403, 2431 (**2008**).
25. C. Premakumara, M. Kakihana, and M. Yoshimura, *Solid State Ionics* 108, 23 (**1998**).
26. M. Kakihana, *J. Sol–Gel Sci. Technol.* 6, 7 (**1996**).
27. M. P. Pechini, *U.S. Patent,* July 1967. No.3. 330. 697
28. E. R. Leite, A. P. Maciel, I. T. Weber, P. N. L. Filho, E. Longo, C. O. P. Santos, A. V. C. Andrae, C. A. Pakoscimas, Y. Manietle, and W. H. Schreiner, *Adv. Mater.* 14, 5 (**2002**).
29. P. Scherrer, *Gottinger Nachrichten* 2, 98 (**1918**).
30. M. M. Viana, T. D. S. Mohallem, G. L. T. Nascimento, and N. D. S. Mohallem, *Brazilian Journal of Physics* 36 (**2006**).
31. C. Wang and J. Y. Ying, *J. Chem. Mater.* 11, 3113 (**1999**).
32. Z. Tang, J. Zhang, Z. Cheng, and Z. Zhang, *J. Materials Chemistry and Physics* 77, 314 (**2002**).
33. J. J. Stickler, S. Kern, A. Wold, and G. S. Heller, *Phys. Rev.* 164, 765 (**1967**).

Received: 11 October 2010. Accepted: 17 November 2010.